Journal of Materials Chemistry B

Accepted Manuscript

ROYAL SOCIETY OF CHEMISTRY

www.rsc.org/materialsB

Journal of Materials Chemistry B

ARTICLE

Monitoring of cell layer coverage and differentiation with the organic electrochemical transistor

Cite this: DOI: 10.1039/x0xx00000x

M. Ramuz,[a$] A. Hama, [a $] J. Rivnay, [a] P. Leleux, and R. M. Owens[a]

Received 00th January 2012,
Accepted 00th January 2012

DOI: 10.1039/x0xx00000x

www.rsc.org/

Electrical, label-free monitoring of cells is a non-invasive method for dynamically assessing the integrity of cells for diagnostic purposes. The organic electrochemical transistor (OECT) is a device that has been demonstrated to be advantageous for interfacing with biological systems and had previously been shown to capable of monitoring electrically tight, resistant, barrier type tissue. Herein, the OECT is demonstrated not only for monitoring of barrier tissue such as MDCK I cells, but also for other, non-barrier tissue adherent cells including HeLa cells and HEK epithelial cells. Transistor performance, expressed as transconductance (g_m) is measured as a function of frequency; barrier tissue type cells are shown to have a more abrupt drop in transconductance compared to non-barrier tissue cells, however both tissue types are clearly distinguishable. Simple modelling of the cell layers on the transistor allows extraction of a resistance term (R_c). OECT monitoring shows that barrier tissue cells lose their barrier function in a standard calcium switch assay, but remain adhered to the surface. Re-addition of calcium results in recovery of barrier tissue function. The entire process is continuously followed both electronically and optically. Finally, high resolution fluorescence imaging of live cells labelled with a red fluorescent actin marker demonstrates the versatility of this method for tracking molecular events optically, with direct correlation to electronic readouts.

Introduction

The development of electrical techniques for monitoring of biological phenomena is a field that is fast gathering pace.[1] Advantages of electrical techniques are manifold, including the fact that they are label-free, and have the potential to be very efficient transducers, since the signal measured is already in an electrical readout format. Electronic methods for live-cell sensing can be applied to applications involving extracellular recording of electrical activity from electrically active cells (neurons/myocytes), but also for monitoring of non-electrically active cells and tissue assemblies.[1] For the latter, electrical impedance sensing (EIS) has emerged as a dynamic method, with potential for high throughput screening for drug discovery or toxicology, and has been demonstrated for use in monitoring cellular adhesion,[2] proliferation,[3] micro motion,[4] wound healing[5] and more.[6, 7] Depending on the format of the impedance sensor, and the method of integration with the cells, different biological phenomena can be observed. Commercially available impedance sensors fall into two categories, the first involves integration with cells grown directly on the electrode surfaces,[8] while in the second cells are grown on semi-permeable membranes.[9] The main difference in these categories is that when cells are grown directly on the electrodes, a cleft resistance arises and also the effective area of the electrode changes as cells cover the electrode.[10] Therefore, adhesion and growth of the cells, as well as differentiation of the cells (e.g. increased resistance due to closer packing) can be monitored. When adherent cells are grown on semi-permeable membranes they are known to polarise, however the only electrical property that can be monitored is the transepithelial resistance (TER), which is the sum of the para and trans-cellular ion flow.[9] TER is a useful parameter for characterising so-called barrier tissue: tightly packed layers of specialised epithelial (and sometimes endothelial) cells whose role is to selectively manage the passage of ions and nutrients into the bloodstream or beyond.[11] The TER is also considered an excellent parameter for assessing tissue integrity, as deteriorations in tissue (e.g. caused by pathogens and toxins) inevitably result in reductions in TER.[12] When grown directly on electrodes, cells may not polarise correctly, however the 'barrier' properties tissues can be still be monitored along with the other parameters such as coverage.[6] In summary, electrical monitoring of cells can be considered as a versatile, dynamic method for readout of biological tissues.

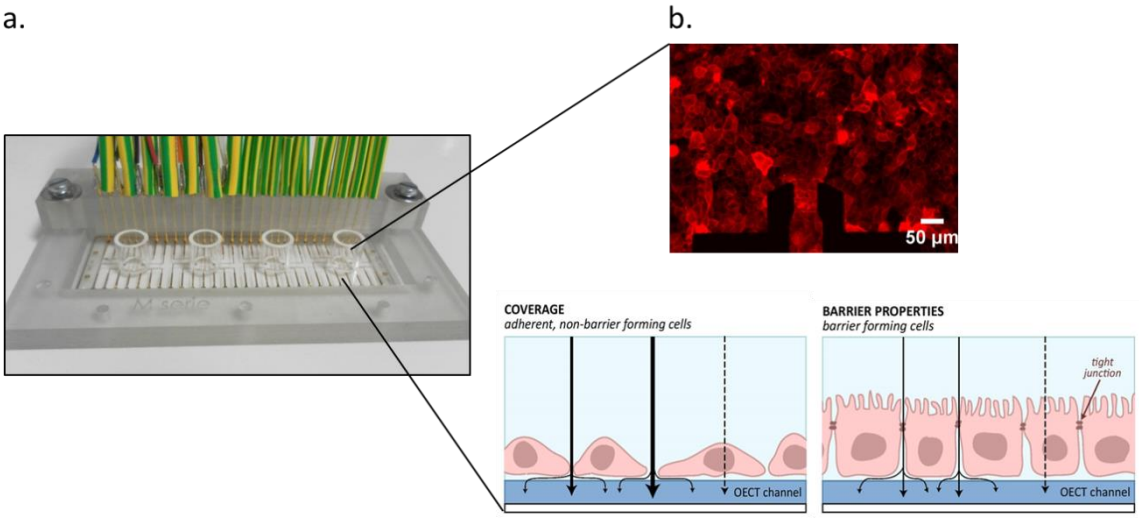

Figure 1. The OECT device used for monitoring adherent cells. a) Picture of the measurement platform which consists of 24 OECTs divided between 4 glass wells. The device is shown inside a 3D printed holder with embedded spring contacts used to probe the OECTs, which sits on a microscope stage. b) Optical fluorescence image (top) of MDCK II cells transfected with RFP actin construct directly seeded on device; and schematic representation (bottom) of the coverage associated with high ion flow through non-barrier forming cell layers (left) or low ion flow through barrier forming cell layers (right). Paracellular –full vertical arrows, transcellular – dashed vertical arrow and sub-cellular-curved arrows, are indicated).

We previously demonstrated the use of the organic electrochemical transistor (OECT) for monitoring the integrity of barrier tissue when grown on semi-permeable membranes.[13] Organic electronic devices in general, and the OECT in particular, have gained significant attention in the last decade as excellent transducers of biological events, due to an array of desirable characteristics including chemical tunability, ease of processing, potential for low cost and compatibility with biological components and systems.[14, 15] Specifically for biosensing, the OECT has been shown to be a very powerful transducer of biological signals,[16] due to a mixed ionic electronic conductivity, allowing direct conversion of ionic signals to electronic ones and vice versa, along with an improved biotic/abiotic interface.[14] The OECT has been used in a wide variety of applications and has proved to be a highly versatile device which can be tailored to each individual biological application.[15] We demonstrated that the OECT was sensitive to minute changes in barrier tissue integrity integrated on permeable membranes, after exposure to a variety of toxins,[17-19] and further, could be used to dynamically monitor infection of tissue by pathogens.[20] We also showed that direct growth of cells on the channel of the device could be used to do combined optical and electronic monitoring, allowing capture of high resolution images of the cells while simultaneously associating electronic data.[21]

To be competitive with commercially available planar EIS devices, the OECT must be capable of monitoring not just barrier tissue but also coverage of any adherent cells on the active area of the device. In this paper we illustrate the power of the OECT to monitor multiple different cell types over time. We show that the OECT is sensitive not only to highly resistant 'barrier' type tissue, but can also be used to monitor other, adherent but non-barrier cell types.

Results and discussion

Previous work using the OECT to monitor live cells was carried out using cells known to have 'tight' barrier tissue properties, with values as high as 2000 Ω.cm² measured using commercially available EIS systems.[22] However, a majority of adherent cells do not have such high resistance even though they may form tightly packed adherent layers on a variety of substrates. To make the OECT more broadly applicable to monitoring adherent cells, we sought to understand the difference between measuring 'tight' cell layers, and 'leaky' cell layers. Previous data had indicated that the adhesion of the cell layers on the active channel of the OECT was modified depending on the type of extracellular matrix protein present, indicating that closer adhesion results in an increase in the cleft resistance.[23] However, this was only in the case of 'tight' cell layers and in the case of cells such as HeLa cells, which are adherent epithelial cells, but not considered barrier tissue, no signal was recorded above background.[21] Improvements in the understanding of the OECT operation,[24] have allowed us to develop devices which can be operated in bandwidth mode, and additionally can be combined with impedance data to generate high quality data across a large spectrum of frequencies.[25, 26] Depending on the input, the temporal resolution can even be in the sub-second regime.[27] In this study we show the use of this new generation of devices to sensitively monitor not only 'tight' barrier tissue, but also 'leaky', non-barrier epithelial cell layers which were hitherto not detectable using the OECT.

Figure 1a shows the devices used in the present study. The use of a microscope equipped with a cell culture incubator allows all measurements to be carried out under physiological

conditions. OECTs are described in the experimental section.Briefly, the dimensions of each OECT are 50 × 50 μm^2. Before seeding, the device was plasma cleaned and sterilized before seeding cells at a concentration of 5×10^4 cells/cm^2. Also illustrated in **Figure 1b**, is the compatibility of the devices with high resolution optical images, not only in bright field but in fluorescence mode. We previously demonstrated that our devices were compatible with immunofluorescence involving fixation of cells on the device at the end of the experiment. In the current study we have generated a transfected epithelial cell line which expresses a red fluorescence protein (RFP) actin gene construct which allows time lapse imaging of live cells in fluorescence mode as illustrated in Figure 1**b**.

To test the new generation of devices for their ability to monitor not just barrier tissue but other adherent cell types, 4 different cell types were used for comparison, all well characterised in literature, with well-understood epithelial phenotypes: MDCK I (Madin Darby Canine kidney epithelial cells) considered to be 'tight' barrier tissue cells,[21] Caco-2 cells – a human colon cancer derived cell line with an intermediate barrier tightness,[18] Hela cells, human cervical cancer derived cells with no known barrier tissue properties and finally HEK 293 cells, human embryonic kidney cell line also with no known barrier tissue properties.[28] Cells were seeded on devices and then monitored for up to 9 days. As recently published, a new figure of merit from this new generation of transistors is used which consists of plotting transconductance (understood as the gain of the transistor) vs frequency.[24]. Compared to classical impedance spectroscopy, this technique allows improving the quality of the recording over the full frequency spectrum and thus increasing the signal to noise ratio.

As seen on Figure 2a, the OECT alone shows a typical profile for a device of this type with a plateau until approximately 1000 Hz when the transconductance drops abruptly. In the case of the leaky cell types, Hela and HEK 293, the cut off is approximately one order of magnitude lower (100-200 Hz), while in the case of Caco-2 and MDCK I cells, the cut off values are another order of magnitude lower (10-50 Hz), following the same trends cited in literature with Caco-2 cells having intermediate resistance and MDCK with very high resistance. The electrical monitoring provided by the OECT thus mirrors that described in literature: HEK 293 and HeLa cells have no barrier tissue properties, while Caco-2 and MDCK I show moderate and high barrier properties respectively. Importantly, the current generation of devices are sensitive not only to barrier tissue but to other 'leaky' adherent cells.

Taking advantage of our ability to monitor the cells in a time-lapse type study, we monitored the 4 cell types MDCK I and Caco2 cells (adherent with barrier properties). and HeLa, and HEK 293 cells (adherent epithelial cells, leaky) continuously for up to 9 days (**Figure 2b**). As demonstrated previously the frequency dependent data can be fit with a simple model (**Figure 2b** inset) to extract parameters such as resistance.[25] By plotting the cell resistance over time we can clearly see the trends followed by the cells, with MDCK I and Caco-2 cells

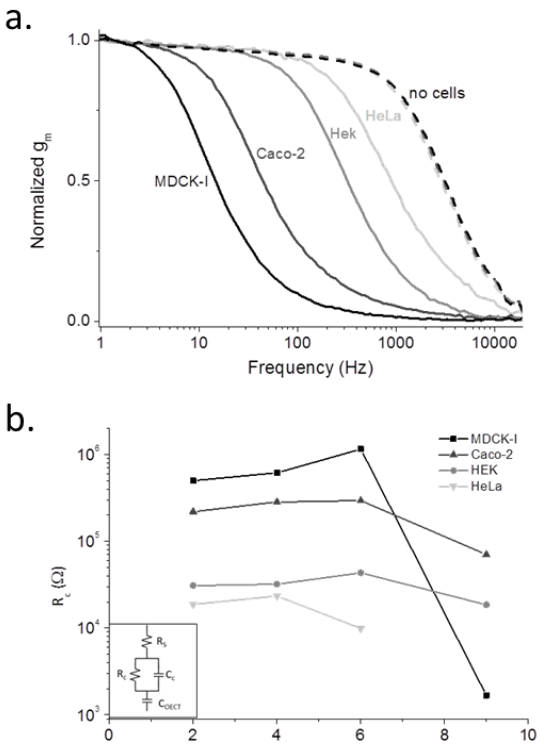

Figure 2. Electrical characterization of Hela, HEK, Caco-2 and MDCK I cells using the OECT. a) Normalized g_m all at day 6, compared with no cells. b) Time course of the cell resistance (R_c) extracted from a simple fit (circuit in the inset) for the different cell lines.

grouped as barrier tissue forming cells, while HEK 293 and HeLa cells are grouped at lower resistances. The faster growth rate of HeLa cells prevented monitoring of this cell type after day 6.

As further proof of our ability to monitor both leaky and tight adherent cells on our devices, we used a calcium switch assay, a standard assay used to monitor barrier tissue function, which can reversibly disrupt barrier formation without detaching cells from the surface.[29] Ca^{2+} is an important component of the adherens junction which plays a role in cell-cell contacts and stabilises the tight junction. Removal of Ca^{2+} is known to disrupt barrier tissue in a manner which can be reversible if the Ca^{2+} is replaced. The Ca^{2+} switch assay using the OECT is shown in **Figure 3**, with the extracted resistance plotted with respect to time.

MDCK I cells were seeded on the devices as before and grown inside the incubator. At day 4, OECTs with the cells were placed inside an AxioObserver Z1 microscope equipped with a humidified incubator and electrical and optical recording was started. Healthy cell layers show a resistance R_c = 3×10^5 Ω (**Figure 3a**). EGTA was added to chelate the Ca^{2+}, resulting in complete loss of the barrier tissue function with a Rc = 4.5×10^{4}Ω which is close to Hela cells (**Figure 2b**). However as shown in the bright field images (**Figure 3b**), the coverage of the MDCK I cells on the device is maintained over the course of the experiment. Removal of the EGTA containing media, and replacement with Ca^{2+} containing media results in the recovery of the barrier tissue function and recovery of the

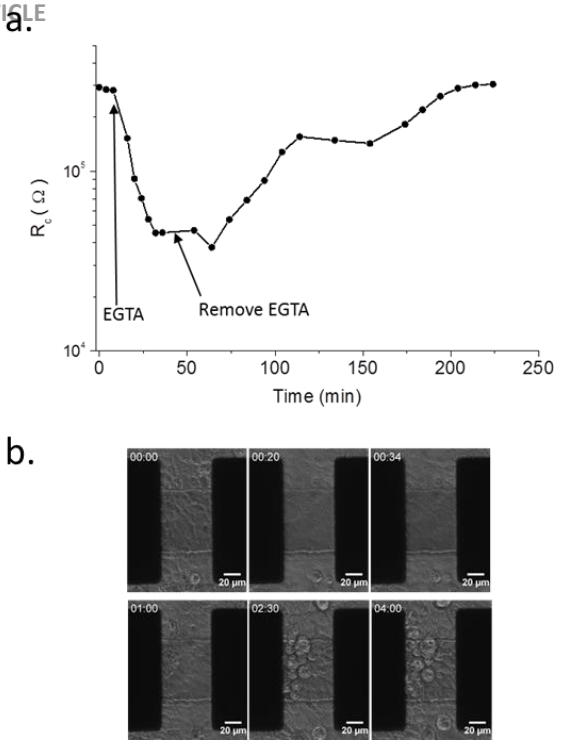

Figure 3. Calcium switch assay using OECTs. a) Extracted resistance plotted vs time. Arrows shows addition of EGTA (100mM) at 11 minutes, and addition of calcium containing media at 40 minutes. b) Images from time lapse with time stamp shown above left; show gold contacts (black) with channel between.

electrical signal to almost initial values after approximately 3 hours (**Figure 3a**). Our system has thus the ability to measure the disruption of the barrier tissue properties by EGTA and its recovery when Ca^{2+} is replaced. We can thus efficiently discriminate between the presence and absence of barrier barrier functionalities (no EGTA) and leaky cell layer state (with EGTA) of MDCK I cells.

One of the key advantages of the OECT compared to commercially available EIS systems, is the ability to take high resolution images in both brightfield and fluorescence modes.[21] This is a distinct advantage over commercial EIS devices using gold or other materials which are incompatible with high resolution imaging, particularly in fluorescence mode.[30] To capitalize on this benefit, we transfected MDCK II cells with a red fluorescent labelled actin construct to specifically follow the expression of actin while simultaneously monitoring the electrical characteristics of the cells. MDCK II are known to be barrier tissue cells, albeit with low TER, around 150 Ω.cm².[31] Attempts to transfect MDCK I cells were unsuccessful, perhaps related to the very tight, closely packed morphology of these cells which may render them refractive to the transfection process.

The time lapse assay was carried out at day 4 as before with the difference that images were collected in both brightfield and fluorescence modes. As expected, addition of high concentrations of EGTA results in a fast decrease of the resistance. Contrary to Figure 3, this experiment focuses on the disruption of the barrier tissue property and also the loss of mechanical properties of the cell layer optically characterized by detachment of the cells. As illustrated here, continued, long term exposure to EGTA at high concentrations not only affect the lateral junctions of the cell layer, but will eventually disrupt the basolateral binding of the cells to the substrate. Fitting the data to the simple equivalent circuit described above, resistance values were extracted (**Figure 4a**). The initial resistance of MDCK II, Rc = $1\times10^5\Omega$, lie in between the R_c of Caco2 and HEK 293 which is perfectly consistent with its TER reported in the literature. A 50% decrease in resistance is seen within 20 minutes using the electrical monitoring. The only change visible from the optical imaging is perhaps a slightly subjective increase in the definition of the cell periphery, which may be as a result of the cells moving slightly apart. However, a clear optical defect is visible by 40 minutes. As seen in the bottom panel of **Figure 4b** the fluorescence images allow easier identification of defects and cell delamination in the tissue layer than the brightfield ones. As mentioned previously, if the calcium is not replaced, not only will the barrier tissue properties is lost, but eventually the adhesion of the cell layer on the substrate begins to be lost.[32] As shown in the inset in **Figure 4b** (bottom) cells are either shrinking or detaching so that visible holes in the tissue layer can be observed.

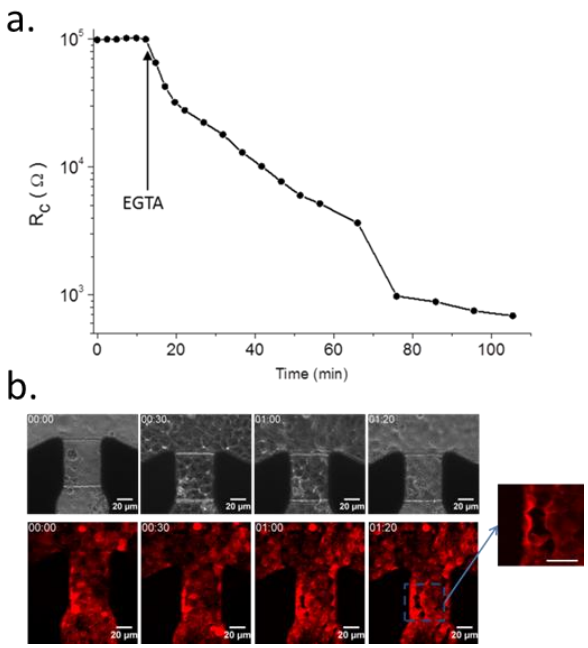

Figure 4. Simultaneous electrical and optical recording of RFP actin labelled MDCK II cells in the presence of EGTA. On a confluent cell layer, EGTA (100mM) was added at t = 13min. a) Extracted resistance plotted vs time. Arrow shows addition of EGTA. b). Corresponding brightfield (top) and fluorescent (bottom) images. A zoom of the blue square in the last fluorescent image highlights the defect visible in the cell layer.

Conclusions

The present studies show the potential of the OECT not only for monitoring barrier tissue cells, but also for monitoring any adherent cell type. This opens up the application of the OECT for studying general toxicology of cells. Parallel work on increasing the temporal resolution of the device and also on integrating the device into non-standard formats (e.g. monitoring cells in 3D cultures) underline the utility of the OECT as a powerful method for studying cell integrity and function. Future work will focus on using other cell lines labelled with other molecular markers such as tight junction proteins to enable correlation of electrical signals more precisely with molecular events.

Acknowledgements

We gratefully acknowledge funding from the European Research Council ERC-2010-StG Proposal No 258966 (IONOSENSE)

Experimental

OECT Fabrication: The conducting polymer formulation consisted of PEDOT:PSS (Heraeus, Clevios PH 1000), with ethylene glycol (Sigma Aldrich, 0.25 mL for 1 mL PEDOT:PSS solution), 4,dodecylbenzenesulfonic acid (DBSA, 0.5 µL/mL), and 3-glycidoxypropyltrimethoxysilane (GOPS) (10 mg/mL). On a clean glass substrate (75 mm x 25 mm), gold source and drain contacts were patterned via photolithography, thermal evaporation, and subsequent lift-off. Photoresist S1813 (MicroChem Corp.) was spin coated at 3000 rpm for 30 s on the glass substrate. Patterns were defined by photolithography (Chrome mask and Mask Aligner). MF-26A was used as developer. Then, 5 nm and 100 nm of chromium and gold respectively, were evaporated. Finally, the photoresist was lifted-off in an acetone bath under sonication for 1 hour, which left the substrate with the source and drain Au contacts only. PEDOT:PSS channel dimensions were patterned using a parylene peel-off technique described previously,[33, 34] resulting in a PEDOT:PSS channel with width and length of 50 µm and 50 µm, respectively, and thickness of 460 nm. A planar gate PEDOT:PSS gate was 1 mm width and 1 mm length.[23] Following PEDOT:PSS deposition, devices were baked for 1 hour at 140°C under atmospheric conditions. Glass wells of 0.64 cm^2 (hole diameter of 0.9 cm) defined the cell growth area.

OECT operation: All measurements were done using the PEDOT:PSS film as gate electrode and cell media (as described below) was the electrolyte. Experiments were performed in a humidified incubator XL multi SI from PECON GmbH mounted on a microscope Axio Observer Z1 from Carl Zeiss MicroImaging GmbH. Temperature and CO_2 level were at 37°C and 5%, respectively. Measurement parameters were chosen to avoid exposing the cell monolayers to a voltage drop above 0.6V, as high voltages have been shown to damage bilayer membranes.[35] The measurements were performed using a National Instruments PXIe-1062Q system. The channel of the OECT (V_{DS}) was biased using one channel of a source-measurement unit NI PXIe-4145. The gate voltage was applied and controlled using a NI PXI-6289 modular instrument. For frequency-dependent characterization of the OECT, we used NI-PXI-4071 digital multimeters to measure simultaneously drain and gate current. The bandwidth measurements were performed by applying a sinusoidal modulation (ΔVgs = 10 mV peak-to-peak, 1 Hz < f < 20 kHz), V_{DS} = -0.6 V , and measuring ΔI_{DS}, and therefore transconductance (gm) as a function of frequency. The recorded signals were saved and analyzed using customized LabVIEW and Matlab software.[27]

Cell Culture: HeLa, Caco-2 and MDCK-I cells were purchased from HPA culture collection). HEK-293 cells were a kind gift from Marc Borsotto (IPMC, Valbonne) and MDCK-II cells were a gift from Frederic Luton (IPMC, Valbonne). The cells were cultivated in DMEM (Advanced DMEM Reduced Serum Medium 1X, Invitrogen) with 2 mM Glutamine (Glutamax™-1, Invitrogen), 10% FBS (Fetal Bovine Serum, Invitrogen), 0.5% PenStrep (PenStrep 100X, Invitrogen) and 0.1% Gentamicin (Gentamicin 100X, Invitrogen). HeLa, Caco-2 and HEK-293 cells were grown in DMEM with high glucose and MDCK-I and MDCK-II were grown in DMEM with low glucose, all at 37°C, 5% CO_2 in humidified atmosphere.

Calcium switch assay: MDCK-I and MDCK-II cells were grown directly on top of the OECT. They were maintained inside the incubator for 4 days to obtain a monolayer of cells. The media was renewed 1 day before the experiment. Then, the substrate bearing the OECTs seeded with cells was placed onto the stage of the microscope (AxioObserver Z1, Carl Zeiss). After 1 hour required for stabilization, the recording of the electrical signal of the OECT and time-lapse optical recording was started with 5 min delay between pictures. After ~15 minutes and while continuing the recording, an appropriate volume of 0.5M EGTA solution (EMELCA Bioscience) was added into the media to obtain the desired concentration. During all measurements the cells were maintain at 37°C in humidified atmosphere with 5% CO_2.

Transfection: MDCK-II cells were plated in 96-well plate (BD Falcon) and transfected with p^{CMV}LifeAct–TagRFP (ibidi GmbH) using Lipofectamine® 3000 in Opti-MEM Reduced Serum Medium. The transfection conditions were in accordance with the Lipofectamine® 3000 reagent protocol (Invitrogen). A clone was selected and cultivated with 500 µg/ml of Geneticin® (Invitrogen) to establish a stable clone having a good expression of fluorescent labelling of actin. cytoskeleton. After amplification the cells were used in time-lapse experiment using a fluorescent microscope (Axio Observer Z1 Carl Zeiss)..

Notes and references

[a] *Department of Bioelectronics, Ecole Nationale Superieure des Mines, CMP-EMSE, MOC, 13541, France. E-mail: owens@emse.fr*
[$] *These authors contributed equally to this work*

1. C. D. McCaig, A. M. Rajnicek, B. Song and M. Zhao, *Physiological Reviews*, 2005, **85**, 943-978.
2. C. R. Keese, J. Wegener and L. Giaever, *Genet Eng News*, 2005, **25**, 42-43.

3. P. Mitra, C. R. Keese and I. Giaever, *BioTechniques*, 1991, **11**, 504-510.
4. I. Giaever and C. R. Keese, *Proc Natl Acad Sci U S A*, 1991, **88**, 7896-7900.
5. C. R. Keese, J. Wegener, S. R. Walker and I. Giaever, *Proc Natl Acad Sci U S A*, 2004, **101**, 1554-1559.
6. K. Benson, S. Cramer and H.-J. Galla, *Fluids and Barriers of the CNS*, 2013, **10**, 5.
7. I. Giaever and C. R. Keese, *Proc Natl Acad Sci U S A*, 1984, **81**, 3761-3764.
8. C. R. Keese, K. Bhawe, J. Wegener and I. Giaever, *BioTechniques*, 2002, **33**, 842-844, 846, 848-850.
9. J. Wegener, D. Abrams, W. Willenbrink, H. J. Galla and A. Janshoff, *BioTechniques*, 2004, **37**, 590, 592-594, 596-597.
10. C. M. Lo, C. R. Keese and I. Giaever, *Exp Cell Res*, 1999, **250**, 576-580.
11. J. M. Anderson and C. M. Van Itallie, *Cold Spring Harbor perspectives in biology*, 2009, **1**, a002584.
12. J. A. Guttman and B. B. Finlay, *Biochimica et biophysica acta*, 2009, **1788**, 832-841.
13. L. H. Jimison, S. A. Tria, D. Khodagholy, M. Gurfinkel, E. Lanzarini, A. Hama, G. G. Malliaras and R. M. Owens, *Adv. Mater.*, 2012, **24**, 5919-5923.
14. J. Rivnay, R. M. Owens and G. G. Malliaras, *Chem Mater*, 2013.
15. X. Strakosas, M. Bongo and R. M. Owens, *J Appl Polym Sci*, 2015, **132**, n/a-n/a.
16. D. Khodagholy, J. Rivnay, M. Sessolo, M. Gurfinkel, P. Leleux, L. H. Jimison, E. Stavrinidou, T. Herve, S. Sanaur, R. M. Owens and G. G. Malliaras, *Nat Commun*, 2013, **4**, 2133.
17. S. Tria, L. Jimison, A. Hama, M. Bongo and R. Owens, *Biosensors*, 2013, **3**, 44-57.
18. S. A. Tria, L. H. Jimison, A. Hama, M. Bongo and R. M. Owens, *Biochimica et biophysica acta*, 2013, **1830**, 4381-4390.
19. S. A. Tria, M. Ramuz, L. H. Jimison, A. Hama and R. M. Owens, *Journal of visualized experiments : JoVE*, 2014, e51102.
20. S. A. Tria, M. Ramuz, M. Huerta, P. Leleux, J. Rivnay, L. H. Jimison, A. Hama, G. G. Malliaras and R. M. Owens, *Adv Healthc Mater*, 2014, **3**, 1053-1060.
21. M. Ramuz, A. Hama, M. Huerta, J. Rivnay, P. Leleux and R. M. Owens, *Adv Mater*, 2014, **26**, 7083-7090.
22. J. D. Dukes, P. Whitley and A. D. Chalmers, *Bmc Cell Biol*, 2011, **12**.
23. M. Ramuz, K. Margita, A. Hama, P. Leleux, J. Rivnay, I. Bazin and R. M. Owens, *Chemphyschem*, 2015, **16**, 1210-1216.
24. J. Rivnay, P. Leleux, M. Sessolo, D. Khodagholy, T. Herve, M. Fiocchi and G. G. Malliaras, *Adv. Mater.*, 2013, **25**, 7010-7014.
25. J. Rivnay, M. Ramuz, P. Leleux, A. Hama, M. Huerta and R. M. Owens, *Appl Phys Lett*, 2015, **106**, 043301.
26. G. C. Faria, D. T. Duong, C. Polyzoidis, J. Rivnay, S. Logothetidis, R. Owens, G. Malliaras and A. Salleo, *MRS Communications*, 2014, **First view**.
27. J. Rivnay, P. leleux, A. Hama, M. Ramuz, M. Huerta, G. Malliaras and R. M. owens, *Scientific reports*, 2015, **in press**.
28. J. Piontek, L. Winkler, H. Wolburg, S. L. Müller, N. Zuleger, C. Piehl, B. Wiesner, G. Krause and I. E. Blasig, *The FASEB Journal*, 2008, **22**, 146-158.
29. M. S. Balda, L. Gonzalezmariscal, R. G. Contreras, M. Maciassilva, M. E. Torresmarquez, J. A. G. Sainz and M. Cereijido, *Journal of Membrane Biology*, 1991, **122**, 193-202.
30. J. Wegener, Phase Contrast & Fluorescence Microscopy of Adherent Cells grown on ECIS Electrodes, http://www.biophysics.com/publications/ECIS_Microscopy_V2_DINA4.pdf.
31. W. J. Armitage, B. K. Juss and D. L. Easty, *Cryobiology*, 1994, **31**, 453-460.
32. J. Wegener, C. R. Keese and I. Giaever, *Exp Cell Res*, 2000, **259**, 158-166.
33. J. A. DeFranco, B. S. Schmidt, M. Lipson and G. G. Malliaras, *Org Electron*, 2006, **7**, 22-28.
34. D. Khodagholy, M. Gurfinkel, E. Stavrinidou, P. Leleux, T. Herve, S. Sanaur and G. G. Malliaras, *Applied Physics Letters*, 2011, **99**, 163304.
35. D. A. Bernards, G. G. Malliaras, G. E. S. Toombes and S. M. Gruner, *Appl Phys Lett*, 2006, **89**, 05305.